Supporting Information

The influence of GaPt droplet purification on the catalytic performance of supraparticles as supported catalytically active metal solutions (SCALMS) in propane dehydrogenation

Philipp Groppe,[a,†] Thomas Zimmermann,[a,b,†] Nnamdi Madubuko,[c] Kevin Bürner,[c] Yaoci Sheng,[d] Christoph Wichmann,[e,f] Michael S. Moritz,[e] Joachim Czechowsky,[g] Valentin Müller,[a,h] Jörg Libuda,[d] Peter Wasserscheid [c,i,j] Karl Mandel,[a] Torben Daeneke,[k] Jan-Dierk Grunwaldt,[g,l] Christian Papp,[e,f] Marco Haumann,[c,m] Tanja Retzer,[d,] Nicola Taccardi,[c,]* Susanne Wintzheimer[a,b,]**

[a]Chair 'Particle-Based Materials Chemistry', Section Materials Chemistry, Department of Chemistry and Pharmacy, Friedrich-Alexander-Universität Erlangen-Nürnberg (FAU), Egerlandstraße 1, 91058 Erlangen, Germany
[b]Fraunhofer-Institute for Silicate Research ISC, Neunerplatz 2, 97082 Würzburg, Germany
[c]Friedrich-Alexander-Universität Erlangen-Nürnberg (FAU), Lehrstuhl für Chemische Reaktionstechnik (CRT), 91058 Erlangen, Germany
[d]Erlangen Center for Interface Research and Catalysis, Friedrich-Alexander-Universität Erlangen-Nürnberg, Egerlandstraße 3, Erlangen 91058, Germany
[e]Lehrstuhl für Physikalische Chemie II, Friedrich-Alexander-Universität Erlangen-Nürnberg (FAU), Egerlandstraße 3, Erlangen 91058, Germany
[f]Angewandte Physikalische Chemie, Freie Universität Berlin, Arnimallee 22, Berlin 14195, Germany
[g]Institute for Chemical Technology and Polymer Chemistry (ITCP), Karlsruhe Institute of Technology (KIT), Engesserstrasse 18, 76131 Karlsruhe, Germany
[h]Chemistry of Thin Film Materials (CTFM), Interdisciplinary Center for Nanostructured Films (IZNF), Department of Chemistry and Pharmacy, Friedrich-Alexander-Universität Erlangen-Nürnberg, Cauerstraße 3, 91058 Erlangen, Germany
[i]Forschungszentrum Jülich GmbH, Helmholtz-Institute Erlangen-Nürnberg for Renewable Energy (IEK-11), 91058 Erlangen, Germany;
[j]Forschungszentrum Jülich GmbH, Institute for a Sustainable Hydrogen Economy (INW), 52428 Jülich, Germany
[k]Department of Chemical and Environmental Engineering, RMIT University, Melbourne, VIC 3001, Australia
[l]Institute of Catalysis Research and Technology (IKTF), Karlsruhe Institute of Technology (KIT), Hermann-von-Helmholtz-Platz 1, Eggenstein-Leopoldshafen 76344, Germany
[m]Research Centre for Synthesis and Catalysis, Department of Chemistry, University of Johannesburg, P.O. Box 524, Auckland Park 2006, South Africa

[†]These authors contributed equally to this work.
*T. Retzer: tanja.retzer@fau.de, N. Taccardi: nicola.taccardi@fau.de; S. Wintzheimer: susanne.wintzheimer@isc.fraunhofer.de

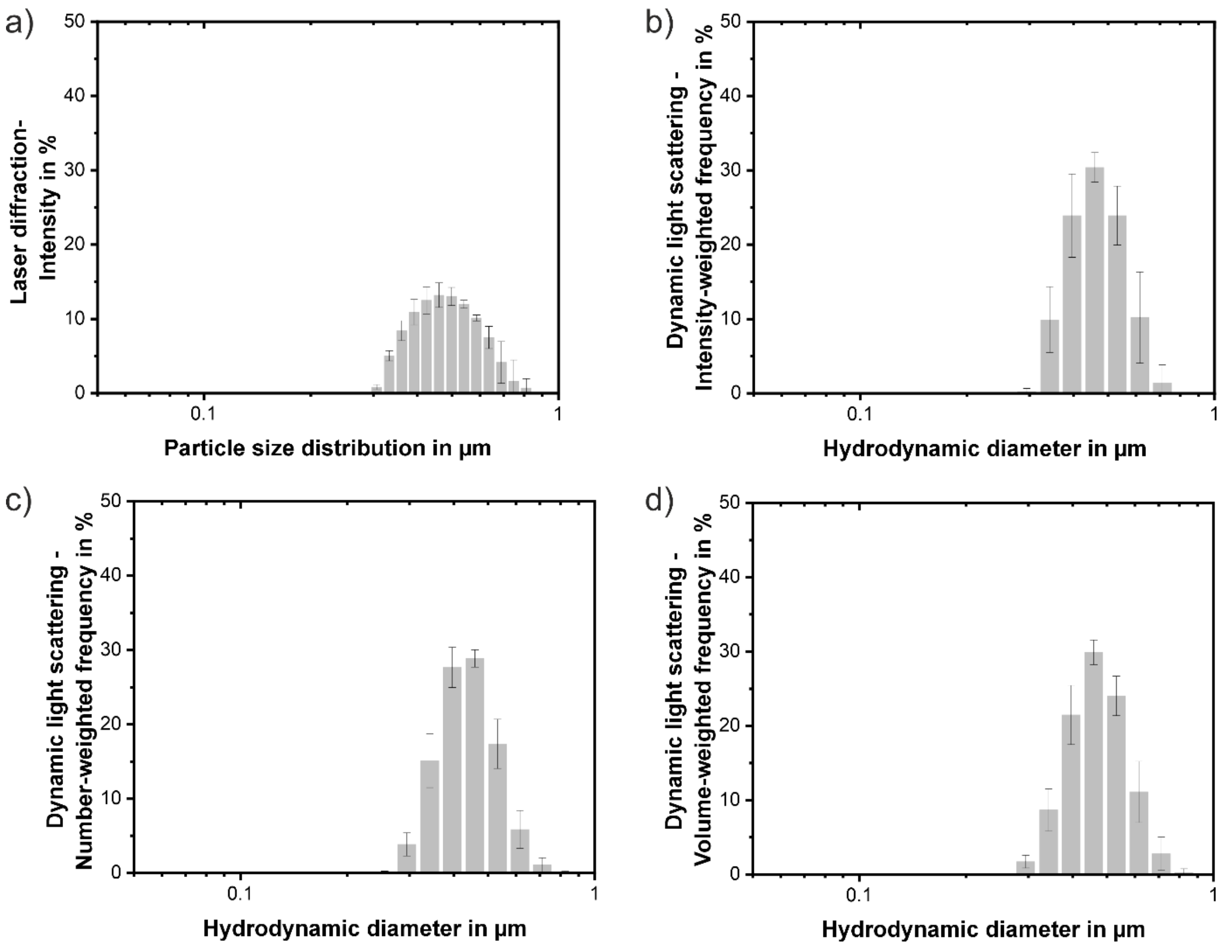

Figure S1. a) Laser diffraction and dynamic light scattering measurements (intensity-, number-, and volume-weighted) of Ga droplets.

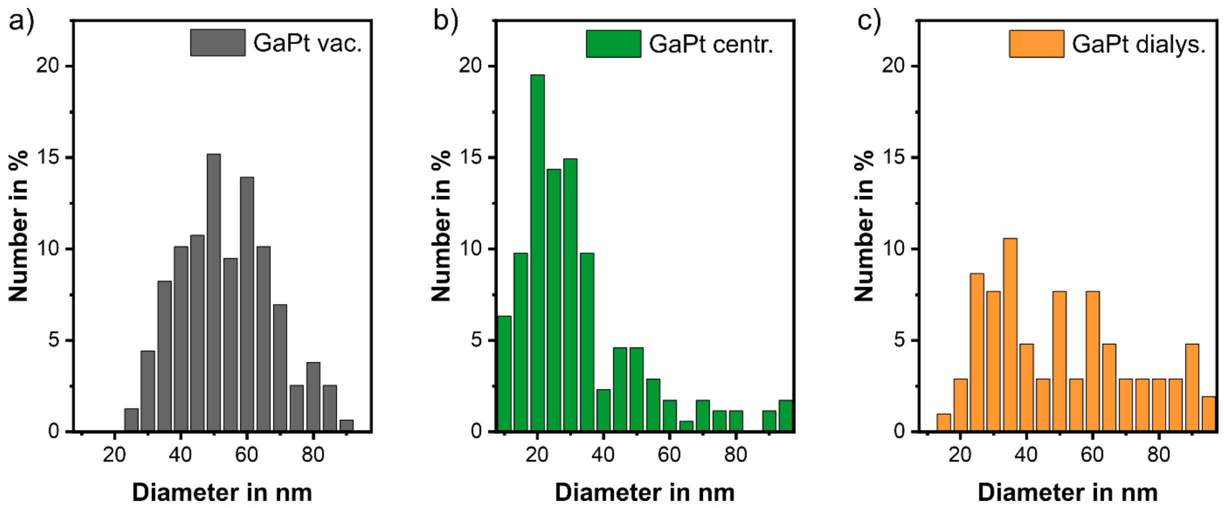

Figure S2. Size of Pt nanoparticles within the nanocomposites: a) GaPt (vac.), b) GaPt (centr.), and c) GaPt (dialys.), determined by measuring 150 Pt nanoparticle diameters in SEM images in backscattered electron contrast.

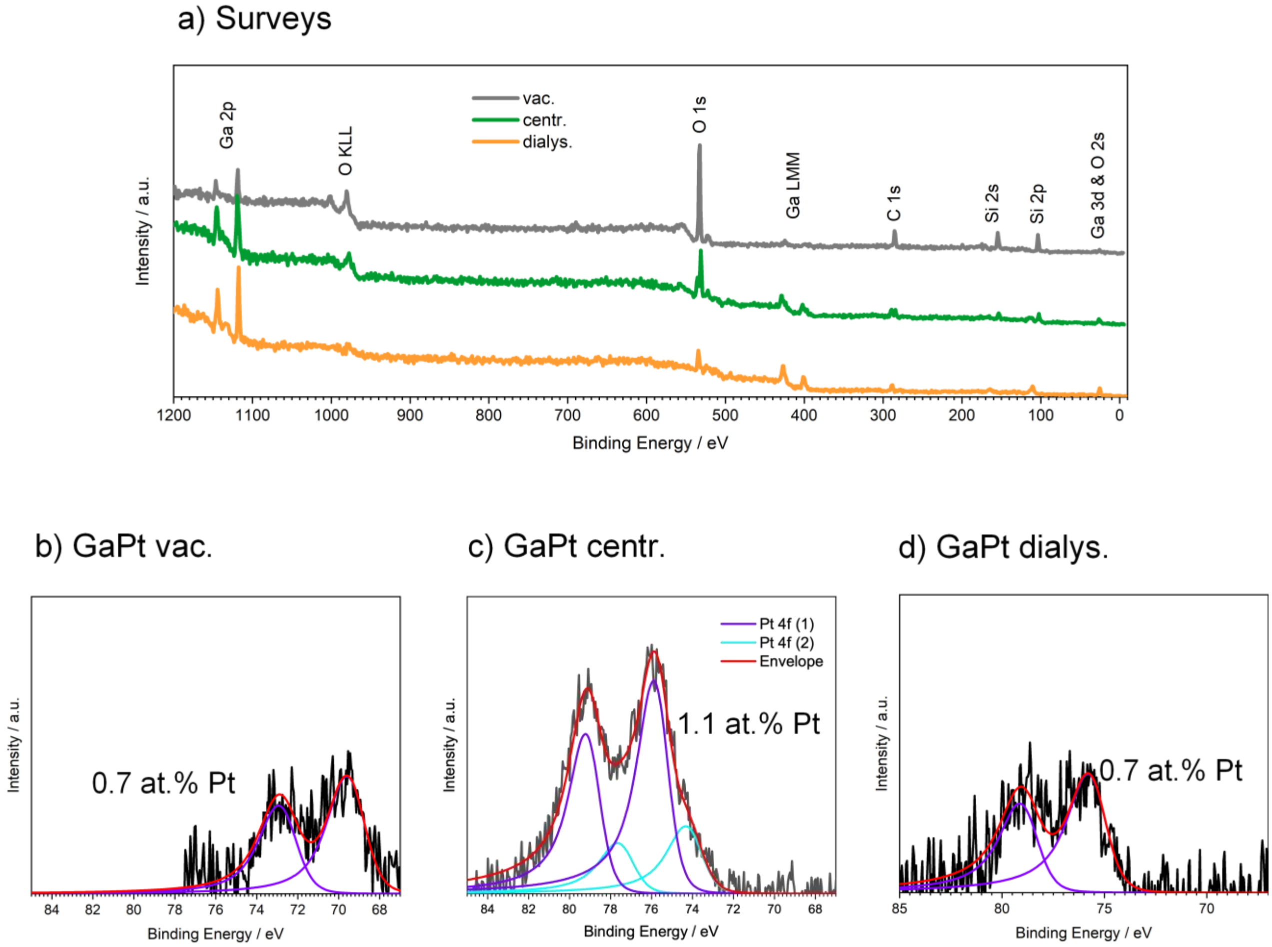

Figure S3. a) Survey XP-spectra and b)-d) fitted XP-spectra of the Pt 4f region. Charging effects result in strong shifts of the position of the signals, which makes a qualitative discussion very difficult. The signals were quantified with respect to the Ga 2p peaks. For GaPt (vac.) and GaPt (dialys.), a Pt content of 0.7 at.% was calculated, while for GaPt (centr.) x_{Pt} is increased to 1.1 at.%.

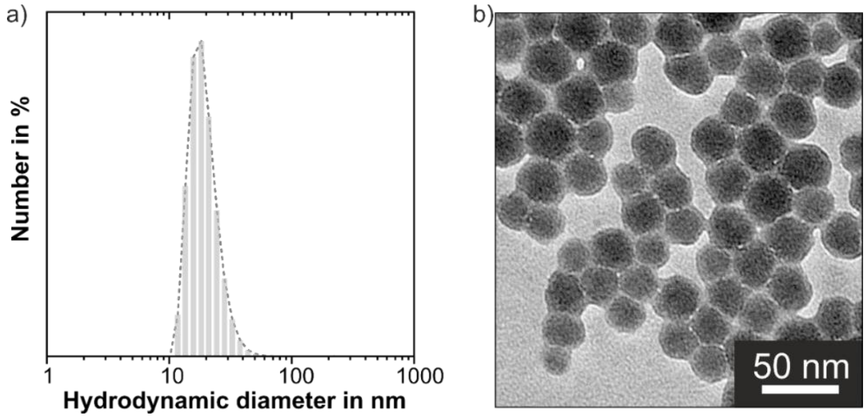

Figure S4. a) Dynamic light scattering measurements and b) TEM of the utilized silica nanoparticles. The mean hydrodynamic size was found to be 18 nm and the measured polydispersity index was 0.15.

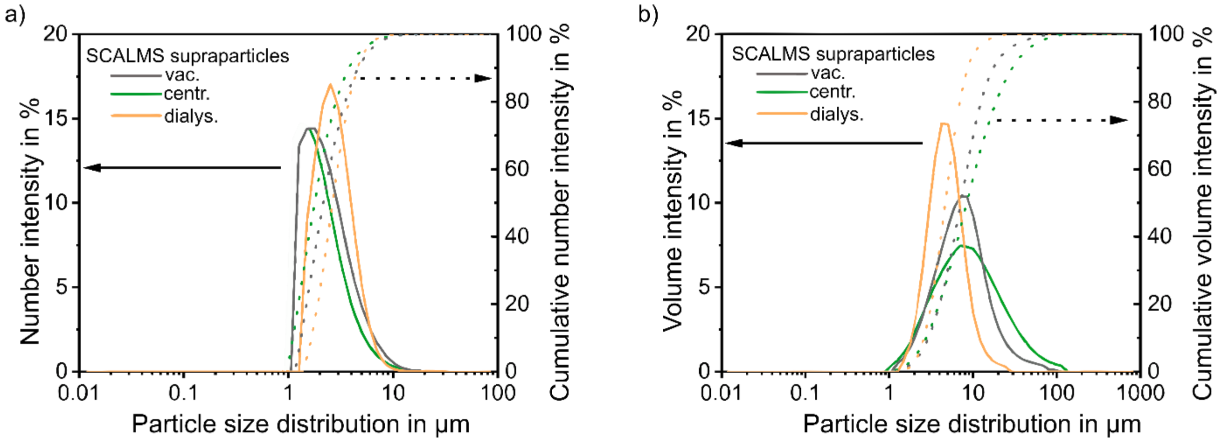

Figure S5. a) Number-weighted and b) volume-weighted particle size distribution obtained from laser diffraction measurements of the synthesized SCALMS supraparticles consisting of silica nanoparticles and GaPt droplets washed via vacuum drying, centrifugation, and dialysis. The size distributions show that all supraparticles samples possess a similar, relatively broad monomodal size distribution.

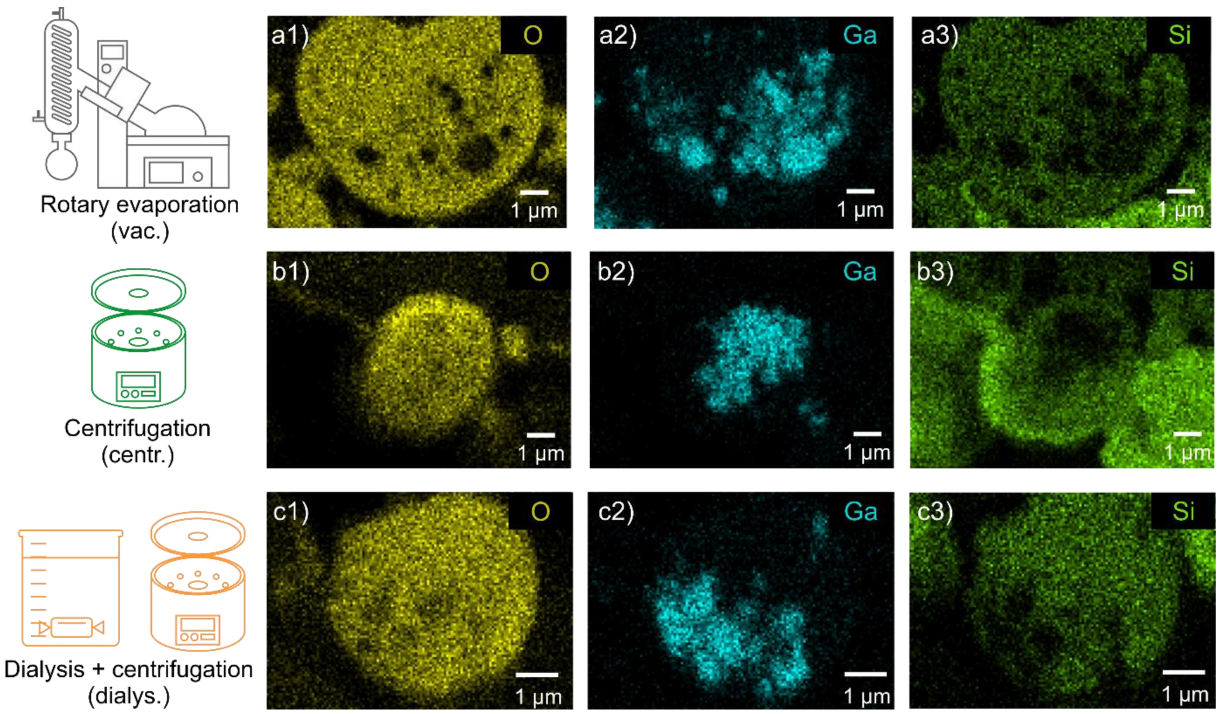

Figure S6. Elemental mappings of SCALMS supraparticle cross-sections containing a) GaPt (vac.), b) GaPt (centr.), and c) GaPt (dialys.).

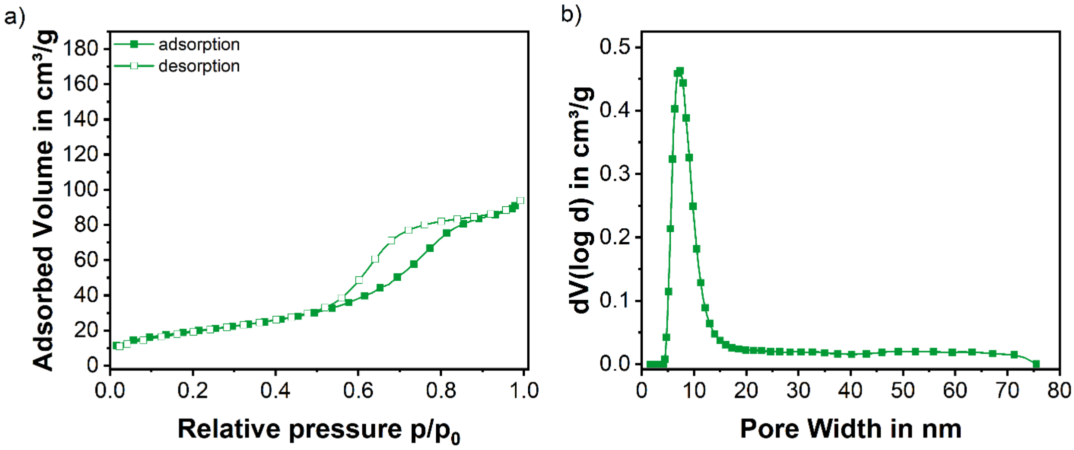

Figure S7. Pore system characterization of SCALMS supraparticles (centr.) consisting of silica nanoparticles and GaPt droplets washed via centrifugation via N_2 sorption at 77 K. a) N_2 isotherms; full symbols represent the adsorption branch and empty symbols the desorption branch. b) Pore size distribution obtained by non-local density function theory (NLDFT).

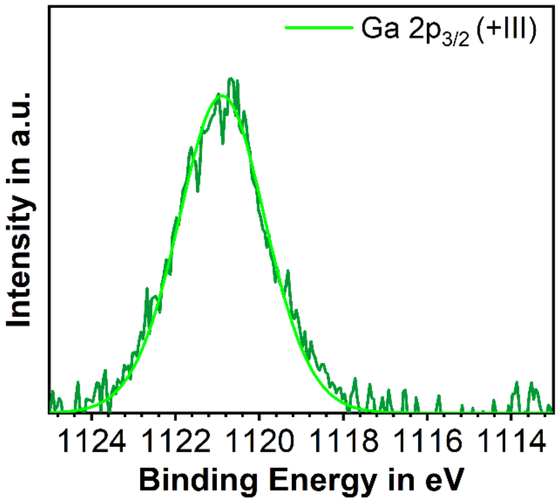

Figure S8. XPS analysis of SCALMS supraparticles (centr.) consisting of silica nanoparticles and GaPt droplets washed via centrifugation. The Ga 2p signal indicates no metallic Ga in the XPS-accessible surface layer of GaPt droplets.

Table S1: Ga wt%, Pt wt%, and Ga:Pt ratio, obtained from ICP-AES analysis of SCALMS supraparticles that were fabricated with increased Pt loading for DRIFTS analyses. The contained GaPt droplets were washed either via rotary evaporation, centrifugation or dialysis.

Sample	Ga in wt%	Pt in wt%	Ga:Pt ratio in $mol_{Ga}\ mol_{Pt}^{-1}$
SCALMS supraparticles (centr.)	27.1	1.5	50:1
SCALMS supraparticles (vac.)	20.2	1.6	35:1
SCALMS supraparticles (dialys.)	9.0	0.9	27:1
Pt/SiO_2 supraparticles as reference	0	1.5	-

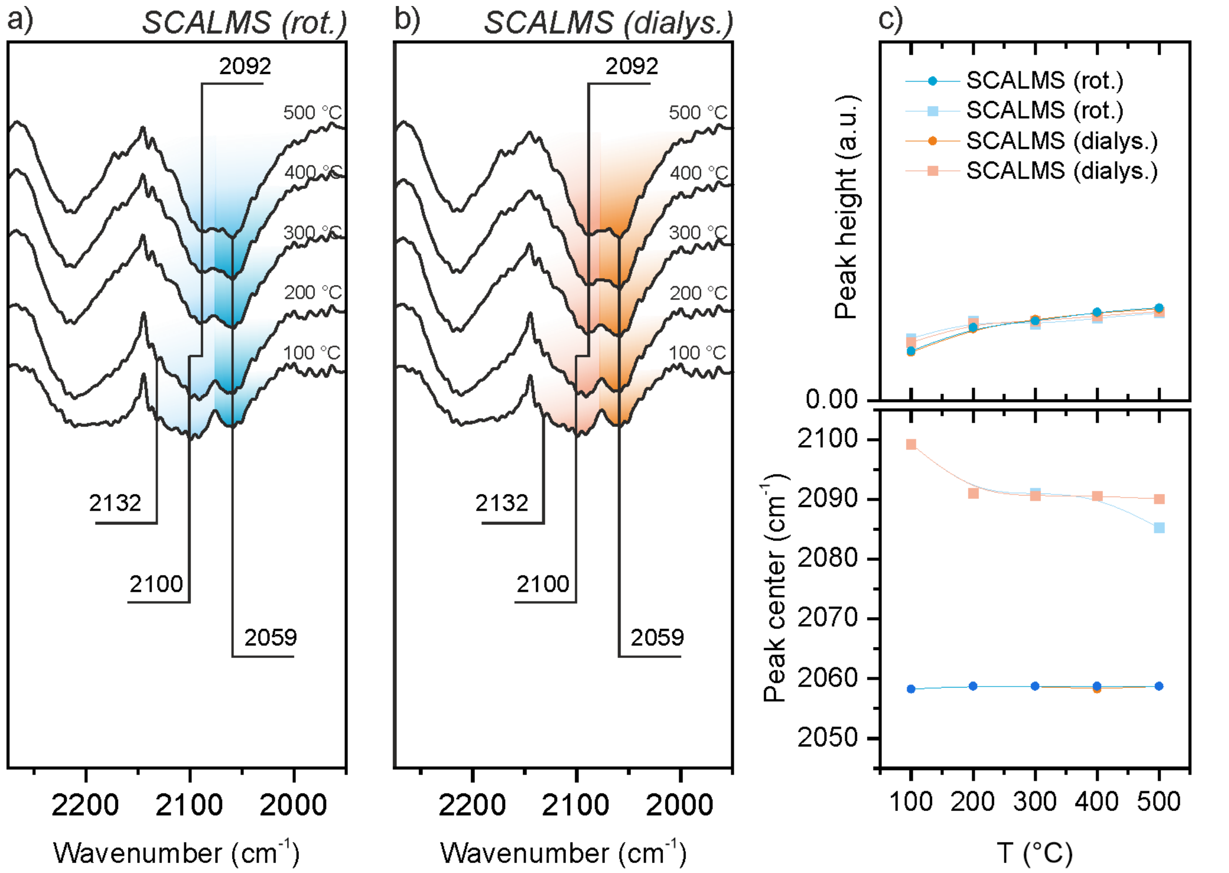

Figure S9. CO-DRIFTS of a) SCALMS supraparticles (rot. = vac.), b) SCALMS supraparticles (dialys.); CO gas phase removed according to [1]; c) Comparison of peak centers and peak heights.

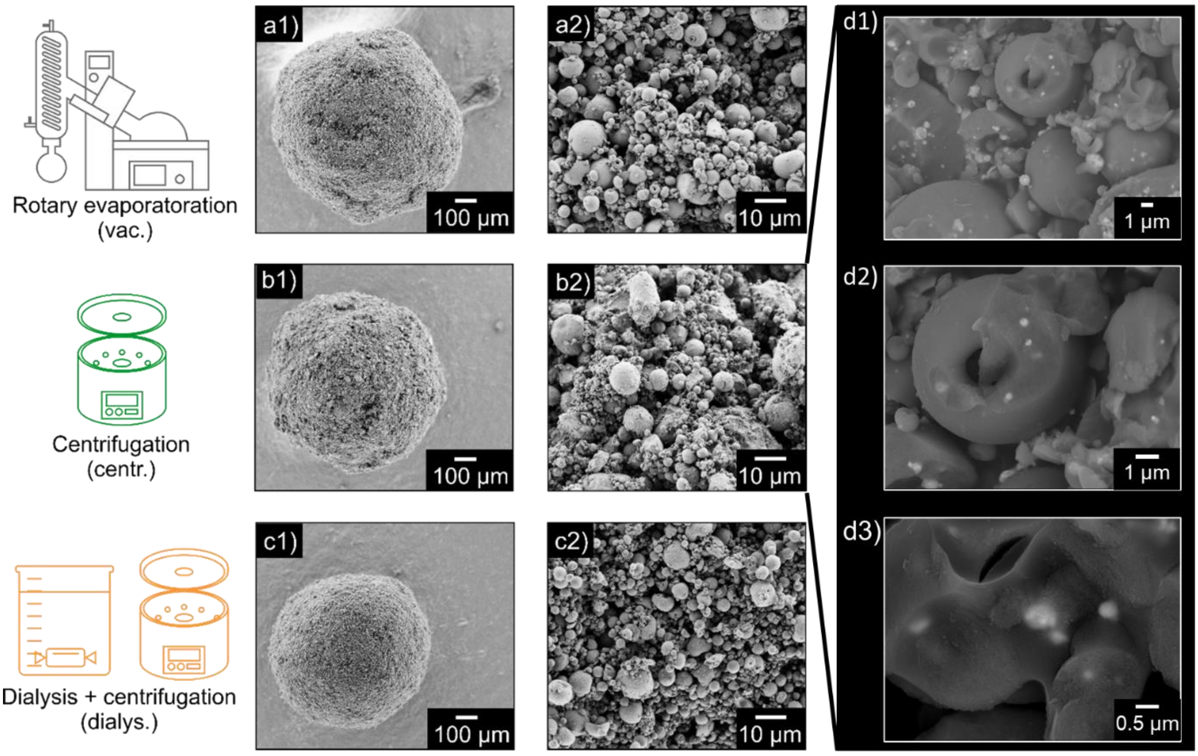

Figure S10. SEM images of SCALMS suprabeads, which contain a) GaPt (vac.), b) GaPt (centr.), or c) GaPt (dialys.) respectively, showing the overview (1) and the detail (2) of each suprabead. d) SEM images in backscattered electron contrast of SCALMS suprabeads containing GaPt (centr.) with increasing magnification (1) to (3).

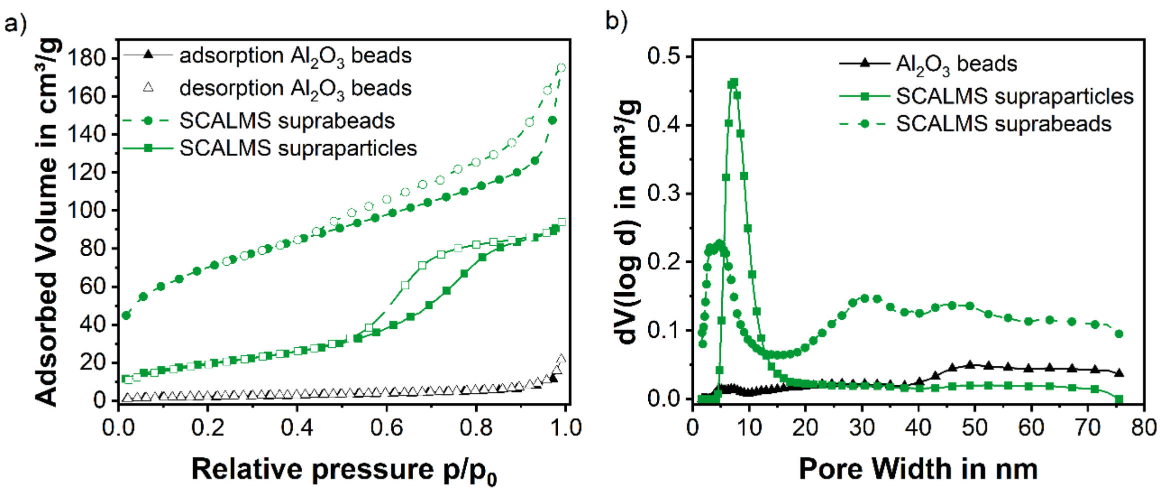

Figure S11. Pore system characterization via N_2 sorption at 77 K of SCALMS supraparticles consisting of silica nanoparticles and GaPt droplets washed via centrifugation, as well as of thereof fabricated SCALMS suprabeads and the Al_2O_3 bead utilized for suprabead fabrication. a) N_2 isotherms; full symbols represent the adsorption branch and empty symbols the desorption branch. b) Pore size distribution obtained by non-local density function theory (NLDFT).

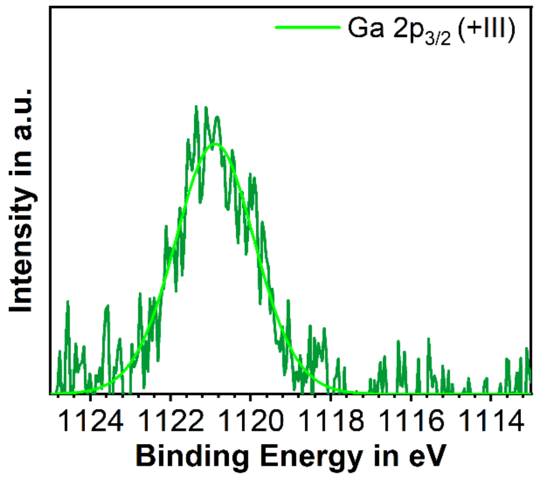

Figure S12. XPS analysis of SCALMS supraparticles consisting of silica nanoparticles and GaPt droplets washed via centrifugation. The supraparticles were oven-treated at 600 °C for 4 h, simulating the thermal stress during suprabead fabrication. The Ga 2p signal indicates no metallic Ga in the XPS-accessible surface layer of GaPt droplets.

Table S2: Ga wt%, Pt wt%, and Ga:Pt ratio, obtained from ICP-AES analysis of suprabeads that were fabricated from supraparticles containing GaPt nanoparticles, which were washed either via rotary evaporation, centrifugation, or dialysis.

Sample	Ga in wt%	Pt in wt%	Ga:Pt ratio in mol_{Ga} mol_{Pt}^{-1}
SCALMS suprabeads (centr.)	2.8	0.1	90:1
SCALMS suprabeads (vac.)	4.3	0.2	82:1
SCALMS suprabeads (dialys.)	2.4	0.1	89:1

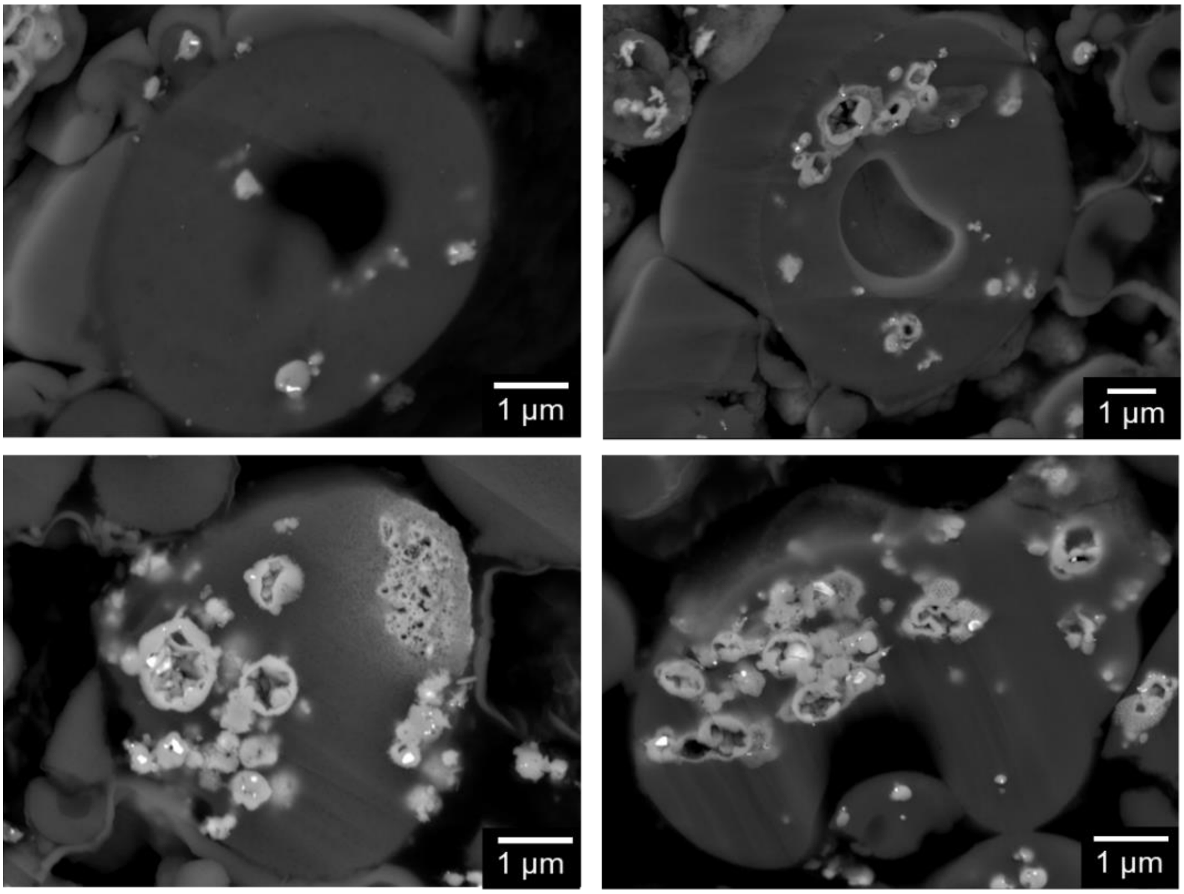

Figure S13. SEM images in backscattered electron mode of SCALMS supraparticle cross-sections containing GaPt (centr.) with focus on the supraparticles at different sample locations.

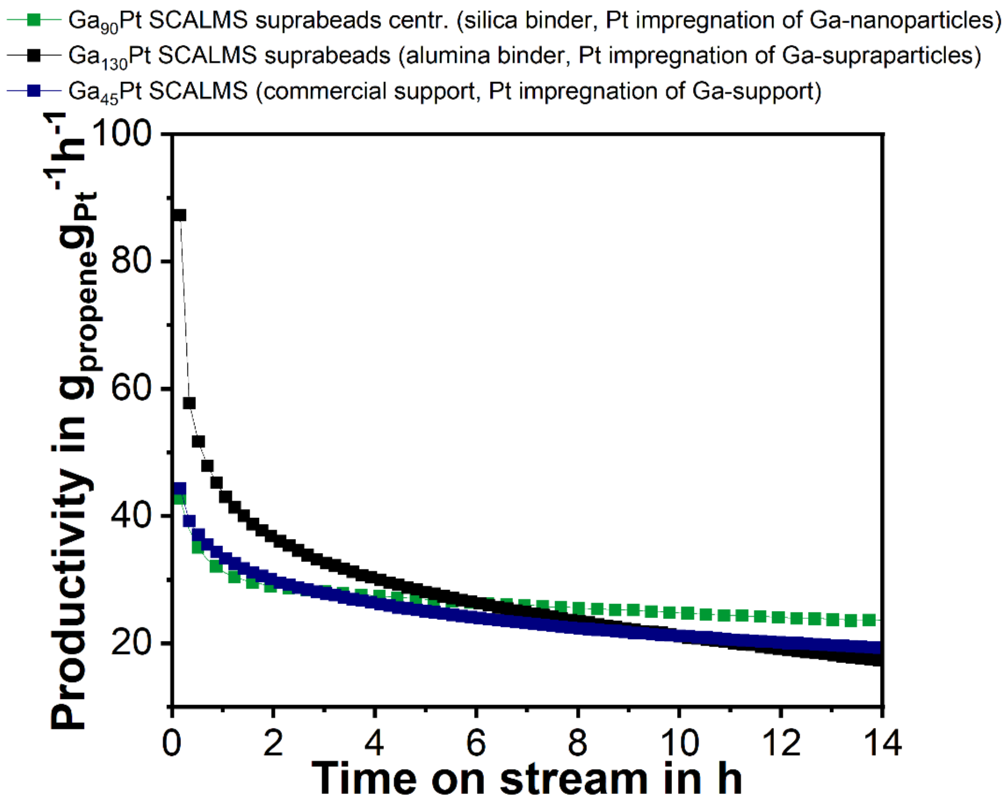

Figure S14. Productivity for SCALMS suprabeads containing $Ga_{90}Pt$ (centr.) as presented in this study in propane dehydrogenation in comparison to former $Ga_{130}Pt$ SCALMS suprabeads,[1] based on an alumina binder, Pt impregnation of Ga-supraparticles, and a Ga to Pt ratio of 130:1, and to $Ga_{45}Pt$ SCALMS based on a commercial support. Catalyst mass in bed, 3 g. Pre-treatment conditions: 19.5 $mL_N\ min^{-1}$ H_2, 80.5 $mL_N\ min^{-1}$ Ar, 1.2 bar, 550 °C. Propane dehydrogenation: 8.9 $mL_N\ min^{-1}$ C_3H_8, 89.9 $mL_N\ min^{-1}$ Ar, 550 °C, 1.2 bar, 15 h TOS, GHSV: 1960 h^{-1}.

Table S3: Summary of the catalytic data of Pt-based catalysts used in propane dehydrogenation reactions (without constant hydrogen gas feed) in the literature (modified from [2]).

Catalyst	Pt in wt%	Temperature in °C	WHSV in h^{-1}	C_3H_8 content in the carrier gas in vol%	Conversion in %	Selectivity in %	Lifetime in h	Formation rate at reaction start in mol C_3H_6 g_{Pt}^{-1} h^{-1} from [2]	Deactivation rate constant in h^{-1} from [2]	Literature
Pt/MCM22-zelite	0.11	550	2.9	91	-	-	-	2.2	-	[3]
Pt/Sn/MFI-zeolite	0.44	450	1.7	24	70-48	90	65	5.5	0.0143	[4]
$Pt/Zn/SiO_2$	2.9	550	75.0	20	30-16	98	60	17.4	0.0271	[5]
$Pt/Ga/Al_2O_3$ SCALMS	0.67	450	-	90	3.6	91	-	-	-	[6]
$Pt/Sn/SiO_2$	3	500	47	20	27-24	99.5	3	9.5	0.0517	[7]
$Pt/Sn/CeO_2$	1	650	2.2	16.7	45-39	78	6	1.7	0.0376	[8]
$Pt/Ga/Mg(Ga,Al)O_x$	3	600	26	20	14-6	98	2.5	2.6	0.3576	[9]
Pt/Sn/MgSBA-15	1	580	8.3	70	43-38	98	6	7.9	0.0339	[10]
$Pt/Ga/SiO_2$	4.37	550	2.0	20	41-38	63.5	20	0.3	0.0046	[11]
Pt/graphene	0.28	600	1.6	5	16-12	88	80	1.9	0.0049	[12]
Pt/carbon nanotubes	3.2	600	1.6	5	10-9	75	20	0.1	0.0111	[13]
Pt_3GaK/Al_2O_3	0.001	620	6.5	100	42-31	97-93	37.5	-	0.0014	[14]
$Pt/Ga/SiO_2/Al_2O_3$ SCALMS suprabeads	0.02	550	-	9	13-3	99-97	15	1.9	0.109[1]	[1]
$Pt/Ga/SiO_2$ SCALMS	0.2	550	-	9	-	99	15	1.0	0.05[1]	[1]
$Pt/Ga/SiO_2$ SCALMS suprabeads	0.01	550	-	9	15-7	98	15	1.0	0.019[1]	this work

[1] Calculated using the formula presented in [15].

4 References

1 T. Zimmermann, N. Madubuko, P. Groppe, T. Raczka, N. Dünninger, N. Taccardi, S. Carl, B. Apeleo Zubiri, E. Spiecker, P. Wasserscheid, K. Mandel, M. Haumann and S. Wintzheimer, Supraparticles on beads for supported catalytically active liquid metal solutions - the SCALMS suprabead concept, *Materials horizons*, 2023, **10**, 4960–4967.

2 S. Chen, X. Chang, G. Sun, T. Zhang, Y. Xu, Y. Wang, C. Pei and J. Gong, Propane dehydrogenation: catalyst development, new chemistry, and emerging technologies, *Chemical Society Reviews*, 2021, **50**, 3315–3354.

3 L. Liu, U. Díaz, R. Arenal, G. Agostini, P. Concepción and A. Corma, Generation of subnanometric platinum with high stability during transformation of a 2D zeolite into 3D, *Nature Mater*, 2017, **16**, 132–138.

4 L. Liu, M. Lopez-Haro, C. W. Lopes, C. Li, P. Concepcion, L. Simonelli, J. J. Calvino and A. Corma, Regioselective generation and reactivity control of subnanometric platinum clusters in zeolites for high-temperature catalysis, *Nature Mater*, 2019, **18**, 866–873.

5 L. Rochlitz, K. Searles, J. Alfke, D. Zemlyanov, O. V. Safonova and C. Copéret, Silica-supported, narrowly distributed, subnanometric Pt-Zn particles from single sites with high propane dehydrogenation performance, *Chemical science*, 2019, **11**, 1549–1555.

6 T. Bauer, S. Maisel, D. Blaumeiser, J. Vecchietti, N. Taccardi, P. Wasserscheid, A. Bonivardi, A. Görling and J. Libuda, Operando DRIFTS and DFT Study of Propane Dehydrogenation over Solid- and Liquid-Supported Ga x Pt y Catalysts, *ACS Catalysis*, 2019, **9**, 2842–2853.

7 L. Deng, H. Miura, T. Shishido, Z. Wang, S. Hosokawa, K. Teramura and T. Tanaka, Elucidating strong metal-support interactions in Pt–Sn/SiO2 catalyst and its consequences for dehydrogenation of lower alkanes, *Journal of Catalysis*, 2018, **365**, 277–291.

8 H. Xiong, S. Lin, J. Goetze, P. Pletcher, H. Guo, L. Kovarik, K. Artyushkova, B. M. Weckhuysen and A. K. Datye, Thermally Stable and Regenerable Platinum–Tin Clusters for Propane Dehydrogenation Prepared by Atom Trapping on Ceria, *Angew. Chem.*, 2017, **129**, 9114–9119.

9 E. A. Redekop, V. V. Galvita, H. Poelman, V. Bliznuk, C. Detavernier and G. B. Marin, Delivering a Modifying Element to Metal Nanoparticles via Support: Pt–Ga Alloying during the Reduction of Pt/Mg(Al,Ga)O x Catalysts and Its Effects on Propane Dehydrogenation, *ACS Catal.*, 2014, **4**, 1812–1824.

10 B. Li, Z. Xu, F. Jing, S. Luo and W. Chu, Facile one-pot synthesized ordered mesoporous Mg-SBA-15 supported PtSn catalysts for propane dehydrogenation, *Applied Catalysis A: General*, 2017, **533**, 17–27.

11 K. Searles, K. W. Chan, J. A. Mendes Burak, D. Zemlyanov, O. Safonova and C. Copéret, Highly Productive Propane Dehydrogenation Catalyst Using Silica-Supported Ga-Pt Nanoparticles Generated from Single-Sites, *Journal of the American Chemical Society*, 2018, **140**, 11674–11679.

12 J. Liu, Y. Yue, H. Liu, Z. Da, C. Liu, A. Ma, J. Rong, D. Su, X. Bao and H. Zheng, Origin of the Robust Catalytic Performance of Nanodiamond–Graphene-Supported Pt Nanoparticles Used in the Propane Dehydrogenation Reaction, *ACS Catal.*, 2017, **7**, 3349–3355.

13 J. Liu, J. Li, J. Rong, C. Liu, Z. Dai, J. Bao, Z. Da and H. Zheng, Defect-driven unique stability of Pt/carbon nanotubes for propane dehydrogenation, *Applied Surface Science*, 2019, **464**, 146–152.

14 J. J. H. B. Sattler, I. D. Gonzalez ‐ Jimenez, L. Luo, B. A. Stears, A. Malek, D. G. Barton, B. A. Kilos, M. P. Kaminsky, T. W. G. M. Verhoeven, E. J. Koers, M. Baldus and B. M.

Weckhuysen, Platinum‐Promoted Ga/Al 2 O 3 as Highly Active, Selective, and Stable Catalyst for the Dehydrogenation of Propane, *Angew. Chem.*, 2014, **126**, 9405–9410.
15 N. Madubuko, U. Sultan, S. Carl, D. Lehmann, X. Zhou, A. Soegaard, N. Taccardi, B. Apeleo Zubiri, S. Wintzheimer, E. Spiecker, M. Haumann, N. Vogel and P. Wasserscheid, Controlled Nanopore Sizes in Supraparticle Supports for Enhanced Propane Dehydrogenation with GaPt SCALMS Catalysts, *ACS Appl. Nano Mater.*, 2024, **7**, 24356–24367.